J Incl Phenom Macrocycl Chem (2009) 64:23–35
DOI 10.1007/s10847-009-9532-y

ORIGINAL ARTICLE

Host–guest system of 4-nerolidylcatechol in 2-hydroxypropyl-β-cyclodextrin: preparation, characterization and molecular modeling

Líllian Amélia Soares · Ana Flávia Vasconcelos Borges Leal · Leonardo Fernandes Fraceto · Elaine Rose Maia · Inês Sabioni Resck · Massuo Jorge Kato · Eric de Sousa Gil · Aparecido Ribeiro de Sousa · Luiz Carlos da Cunha · Kênnia Rocha Rezende

Received: 13 November 2008 / Accepted: 5 January 2009 / Published online: 20 January 2009

Abstract The interaction of 4-nerolidylcatechol (4-NRC), a potent antioxidant agent, and 2-hydroxypropyl-β-cyclodextrin (HP-β-CD) was investigated by the solubility method using Fourier transform infrared (FTIR) methods in addition to UV–Vis, ^{1}H-nuclear magnetic resonance (NMR) spectroscopy and molecular modeling. The inclusion complexes were prepared using grinding, kneading and freeze-drying methods. According to phase solubility studies in water a B_S-type diagram was found, displaying a stoichiometry complexation of 2:1 (drug:host) and stability constant of 6494 ± 837 M^{-1}. Stoichiometry was established by the UV spectrophotometer using Job's plot method and, also confirmed by molecular modeling. Data from ^{1}H-NMR, and FTIR, experiments also provided formation evidence of an inclusion complex between 4-NRC and HP-β-CD. 4-NRC complexation indeed led to higher drug solubility and stability which could probably be useful to improve its biological properties and make it available to oral administration and topical formulations.

Keywords 4-Nerolidylcatechol · 2-Hydroxypropyl-β-cyclodextrin · Inclusion complex · ^{1}H-NMR and molecular dynamics

L. A. Soares · A. F. V. B. Leal · E. de Sousa Gil · L. C. da Cunha · K. R. Rezende (✉)
Laboratório de Biofarmácia e Farmacocinética, Faculdade de Farmácia, Universidade Federal de Goiás, Praça Universitária, 1166. Setor Universitário, 74605-220 Goiânia, GO, Brazil
e-mail: kennia@farmacia.ufg.br

L. F. Fraceto
Departamento de Engenharia Ambiental, Universidade Estadual Paulista, Sorocaba, SP, Brazil

E. R. Maia · I. S. Resck
Instituto de Química, Universidade de Brasília, Brasília, DF, Brazil

M. J. Kato
Departamento de Química Fundamental, Instituto de Química, Universidade de São Paulo, São Paulo, SP, Brazil

A. R. de Sousa
Instituto de Quimica, Universidade Federal de Goiás, Goiânia, GO, Brazil

Introduction

4-Nerolidylcatechol (4-NRC) (Fig. 1a) is the major secondary metabolite from *Pothomorphe umbellata* L. Miq. (Piperaceae), which is known, in Brazil, as "caapeba" or "pariparoba". Their role as a potent antioxidants and, consequently, in the prevention of photodamage has received a great deal of attention lately [1–4], including a patent application claiming for the plant extract on UVB photoprotection [5]. Other pharmacological properties of 4-NRC comprise analgesic and anti-inflammatory action [6], antimicrobial [7] and cytotoxic activity [8] showing a protective genototoxic effect against cyclophosphamide [9]. However, the therapeutic usefulness of the catechol is limited by its unfavorable physicochemical properties, such as its very poor water solubility, in addition to its photosensitivity, making them a challenge to undertake.

Inclusion complexation with cyclodextrins (CDs) has been widely used to improve the solubility and dissolution rate of poor-soluble water drugs [10–12]. Among the CDs, β-CD and HP-β-CD, a hydrophilic derivative (Fig. 1b), are the first choices as they have suitable cavity sizes and relatively low costs. HP-β-CD deserves special attention because of its higher aqueous solubility, lower toxicity as well as a more hydrophobic cavity compared to the parent

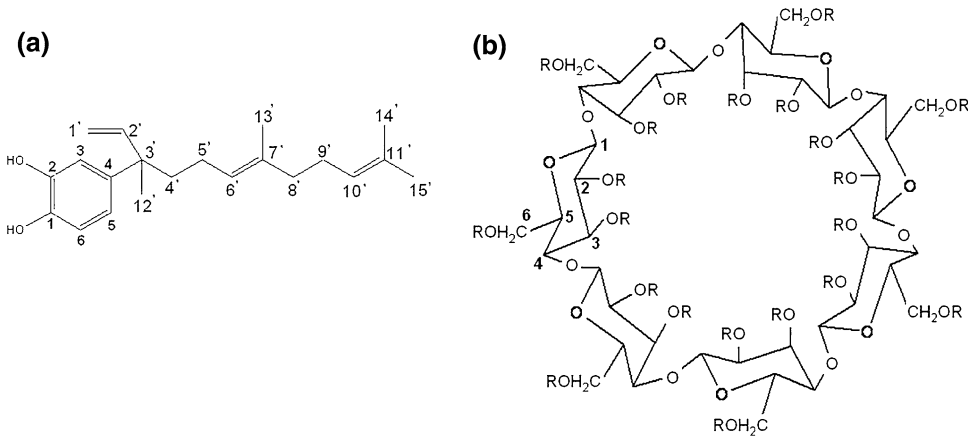

Fig. 1 **a** Chemical structure of 4-NRC. **b** HP-β-CD (R=H or isopropyl group): schematic representation

compound [13–15], making this CD a choice for incorporation of lipophilic molecules into a CD cavity.

Chemically, lipophilic guest compounds are capable of forming stable complexes with properly sized drug molecules. The binding forces within these complexes may involve hydrophobic, van der Waals interactions, hydrogen bonding, or dipole interactions [16].

In our previous work [17], pure 4-NRC could be solubilized up to about 2.5 mg/mL, using a 30% HP-β-CD solution. However, no further details were investigated about the chemical structure, stability or kinetics properties of the complex. The formation of the complex between 4-NRC and HP-β-CD would probably increase the aqueous solubility, stability, bioavailability and mainly it could improve skin permeation of 4-NRC, allowing their use in various pharmaceutical forms, including for oral administration or topical formulations.

Therefore, the aim of this study was to investigate and characterize the interactions between 4-NRC and HP-β-CD in the inclusion complex, and also, to study the stoichiometry and the topology of the obtained complex.

Experimental

Reagents and 4-nerolidylcatechol (4-NRC) isolation

4-NRC was obtained from the crude *Pothomorphe umbellata* L. Miq. ethanolic roots extract, as previously described [9, 17, 18]. Drug purity grade was assessed by HPLC-PDA, according to a validated method (manuscript in preparation), and characterized by spectroscopic analysis (UV, MS, and ^{1}H and ^{13}C NMR, data not shown). HP-β-CD was purchased from Sigma-Aldrich Chemical Company (averaged MW $\sim$1,380 and degree of substitution: 0.8, Milwaukee, USA). Methanol and acetonitrile were of HPLC grade (Tedia Company, USA). All the other reagents were of analytical grade. Deionized water was used throughout the experiments (Mili-Q, Millipore, USA).

Preparation of the 4-NRC/HP-β-CD solid binary systems

Physical mixtures were obtained by mixing 4-NRC (oil) and HP-β-CD powder by simple blending them in a glass mortar, at the same molar ratio (1:1).

Kneading product was prepared at stoichiometric quantities of 4-NRC and HP-β-CD (1:1 molar ratio) by grinding them with a small amount of ethanol: water (1:1) mixture. The slurry was kneaded for 60 min and then dried under vacuum at 39 $\pm$ 1 °C. Next, the product was frozen and lyophilized.

Freeze-dried product was prepared by adding different concentrations (0.0–50.0 mM) of HP-β-CD aqueous solutions to 10 mL stoppered borosilicate glass flasks containing equal amounts of the 4-NRC (1.0 mg). The mixtures were stirred using an orbital multipoint magnetic shaker over a period of 3 days, at 23 $\pm$ 1 °C and protected from light. Each experiment was carried out in triplicate samples. After equilibrium had been reached, samples of each flask were filtered through a Millipore membrane (0.45 μm), frozen and freeze-dried over 24 h in a Freezone 4.5 Labconco® system.

Characterization of the solid binary systems

Phase solubility studies

Phase solubility studies were performed in aqueous medium as described by Higuchi and Connors [19]. HP-β-CD aqueous solutions of different concentrations (0.0–50.0 mM) were added to individual borosilicate flasks (10 mL) containing equal amounts of 4-NRC (1 mg) covered with aluminum foil to protect from light exposure. Triplicate samples were shaken over a period of 3 days, at 23 $\pm$ 1 °C using a multipoint magnetic stirrer. After equilibrium had been reached, the content of each flask was filtered through a PTFE membrane 0.45 μm (Millipore, São Paulo, Brazil). All samples were analyzed by high

performance liquid chromatography (HPLC) under the following conditions: a Varian ProStar 210 equipment coupled to a UV detector 340 set at 282 nm, using a RP-18 Synergi Fusion® column (4μ, 150 × 4.6 mm) from Phenomenex (Torrance, USA) and, methanol: acetonitrile: trifluoroacetic acid 0.1% (62:20:18 v/v, 1.0 mL/min), as mobile phase. *The stability constant* (K_c) was calculated from the linear and ascendant portion of the phase solubility diagram (Fig. 2a) according to Eq. 1 [19]:

$$K_a = \frac{slope}{S_0(1 - slope)} \quad (1)$$

where, *slope* is the value found on the linear regression and S_0 is the intrinsic aqueous solubility of the 4-NRC, determined in the absence of HP-β-CD.

Stoichiometry of the complex

Stoichiometry of the complex was assessed by the continuous variation method using UV–Vis spectrometry [20]. UV spectra were obtained for a series of 4-NRC: HP-β-CD mixtures. The total concentration of guest and host molecule were kept constant (2 mM) but varying the molar ratio fraction of each component from 0 to 1. An analogous set of solutions containing only 4-NRC was prepared in methanol for the drug calibration curve. The absorbance of free 4-NRC in methanol was determined, as a control, and each solution was measured in triplicate. Spectra were recorded using a Varian Cary 50 spectrophotometer and a quartz cell with optical path length of 1.00 cm, at 282 nm, at room temperature.

Fourier transform infrared (FT-IR)

FT-IR spectral studies were carried on a BX/RX Perkin Elmer 60508 model using the KBr disc method (hydraulic press Perkin Elmer 4037). Scanning was carried out from 4,000 to 400 cm^{-1}. The FT-IR spectra of binary complexes were compared with their physical mixture, and with pure HP-β-CD and 4-NRC [21].

^{1}H-NMR

One-dimensional spectra were recorded on a Varian Inova 500 MHz spectrometer. Unbuffered deuterated water (D_2O) was used as the solvent system. Typical acquisition parameters consisted of 16 K points covering a sweep width of 4998.14 Hz, digital zero filling to 128 K and a 0.5 Hz exponential function were applied to the FID before Fourier transformation. The resonance at 4.75 ppm due to residual solvent, present as impurities (H_2O and HDO), was used as internal reference at 298 K. The data were collected without an external reference to avoid possible interactions with the HP-β-CD.

Molecular modelling

The inclusion complexes of 4-NRC in HP-β-CD have been investigated by the docking approach, essentially by molecular mechanics and molecular dynamics. However, for calculations accuracy, and for a better understanding about molecular behavior, in terms of stability and flexibility, the compounds were firstly studied separately, than a 1:1 stoichiometry was considered for the inclusion process to, finally, come to the 2:1 proportion. The simulations were performed using the Accelrys' program-package *Materials Studio (MS) version 4.2* [22]. Molecular mechanics calculations were carried out using Discover version 2007.1 with PCFF force field [23, 24], through the conjugate gradient (Polak-Ribiere) algorithm. Energy minimizations were performed until a maximum derivative of 1.0×10^{-4} kcal mol^{-1} $Å^{-1}$.

Molecular dynamics trajectories were observed at 298 K, under *vacuum*. A good compromise for the equilibration period was 200 ps, for single structures, and for the complexes, with a time step of 1 fs and a cut-off equal to 9.5 Å. When a 4-NRC dimer was introduced into HP-β-CD cavity, fixed constraints were imposed to that structure, in order to avoid unexpected structural distortions. Energy minimizations were performed to permit guest adjustments into the host cavity. After strong steric hindrance corrections, the constraints were removed and the systems were freely reoptimized, before being submitted to dynamics simulations.

The β-cyclodextrin structure (β-CD) was extracted from the Protein Data Bank (PDB code: 1DMB; resolution: 1.8 Å) [25, 26], where the cyclomaltoheptaose (β-CD) was complexed with the maltodextrin binding protein (MBP) [27]. The hydrogen atoms and the hydroxypropyl chains were added to the crystal atomic coordinates set in order to have the HP-β-CD structure. The 4-NRC guest was built by MS/Build tools. Molecular systems were optimized as described above. After fluctuation analysis, the chosen models were resubmitted to molecular mechanics optimization, giving us, for each model, an order of relative potential energies. For each result the Connolly surface area [28, 29] and the occupied volume were calculated. Special attention was given to HP-β-CD surfaces in order to quantify the structural distortions due to 4-NRC inclusion.

Results and discussion

Phase solubility studies

One important pharmaceutical application of CDs is to enhance drug solubility in aqueous solutions. In this work,

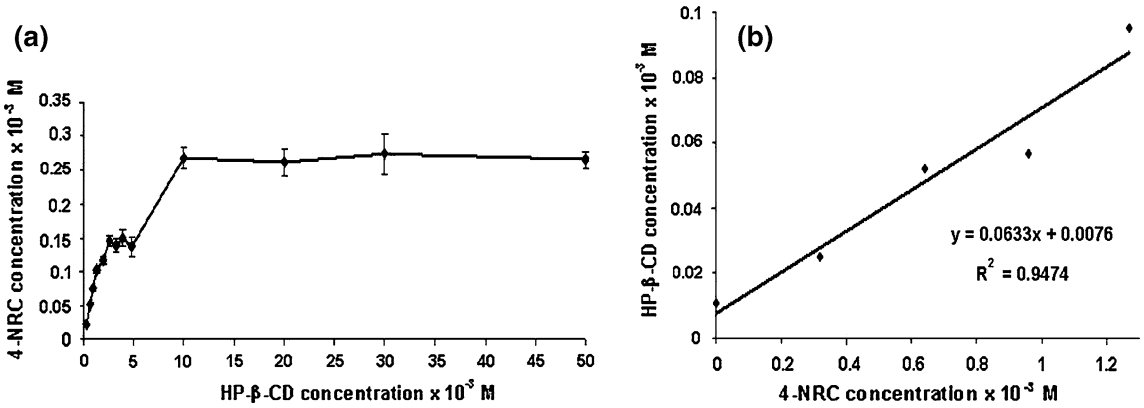

Fig. 2 **a** Phase solubility diagram for 4-NRC at increasing HP-β-CD concentration, determined at 23 °C. **b** Linear part of the phase-solubility diagram for 4-NRC at increasing HP-β-CD concentration, determined at 23 ± 1 °C

the 4-NRC solubility was assessed as a function of HP-β-CD concentration showing a nonlinear process where the drug solubility increases with a negative deviation from linearity (Fig. 2a). Accordingly to Higuchi and Connors [19], such a phase solubility diagram characterizes a B_S type solubility profile.

The determination of the apparent stability constant (K_a) between the drug and CD is based on the index measurement of the changes in physicochemical properties of a compound upon inclusion. Most determining methods of the K_a values are based on an analysis of concentration dependencies, using titration experiments of the drug molecule with the CDs [30]. In this work, the K_a was calculated from the initial linear part (Fig. 2b) of the phase-solubility diagram [19]. Importantly, equilibrium was reached and the complex drug-CD stability constant could be calculated. The intrinsic solubility (S_0) of 4-NRC in water was found to be 1.06×10^{-2} mM (3.32 μg/mL). Subsequently, the apparent stability constant was calculated (6,494 ± 837 M^{-1}) confirming a highly stable complex formation, as previously reported for other similar catechol molecules [31, 32].

According to Blanco et al. [33] and Pitta et al. [34], only complexes showing K_a values between 200 and 5,000 M^{-1} have practical applications. It means that, complexes showing $K_a < 200$ M^{-1} are generally very labile exhibiting premature drug liberation profile or, instead, they are very stable ($K_a > 5{,}000$ M^{-1}) displaying an incomplete or very slow drug release rate. Therefore, the K_a value found in this work (6494 ± 837 M^{-1}) fell outside the practical range. Conversely to previously cited articles, some other authors [35] have shown practical applicability of those inclusion complexes, which may contribute to improving the stability of catechol molecules and, also, the bioavailability of the poorly water-soluble drugs. It should also be pointed out that preliminary data, under investigation with a collaborative research group, has shown higher anticancer activity for 4-NRC inclusion complex than pure compound (manuscript in preparation), corroborating previously cited *Pothomorphe umbellata* crude extract bioactivity [36].

Taking into account the above mentioned 4-NRC aqueous solubility (intrinsic) and, its solubility after experimental addition of HP-β-CD (0.27 mM) (Fig. 2), we found it 26 times higher than the original one (3.3 vs. 85.8 μg/mL), highlighting the importance of the presence of HP-β-CD, and the use of the inclusional technique in the discovery and development of new drugs.

Characterization of inclusion complexes

Stoichiometry of the complex

The stoichiometry of the complex was investigated by continuous variation method (Job's plot) by means of UV–Vis spectrometry observations [37]. The difference of absorbance (ΔA) of 4-NRC with and without HP-β-CD was measured at 282 nm and 21 ± 2 °C. Figure 3 represents a Job's plot of ΔA × r as a function of $r = m/(m + n)$ where m and n are the molar ratios of 4-NRC and HP-β-CD, respectively. The plot shows a maximum value at $r = 0.67$, corresponding to 2:1 (4-NRC: HP-β-CD) stoichiometry.

Fourier transform infrared spectroscopy

Fourier transform infrared spectroscopy (FT-IR): The inspection of the HP-β-CD spectrum (Fig. 4a) shows high intensity bands centered at 3,400 cm^{-1}, related to free –OH groups stretching vibrations, while the pure 4-NRC spectrum (Fig. 4b) also shows free –OH group centered at 3,500 cm^{-1} besides more characteristic as C=C olefinic

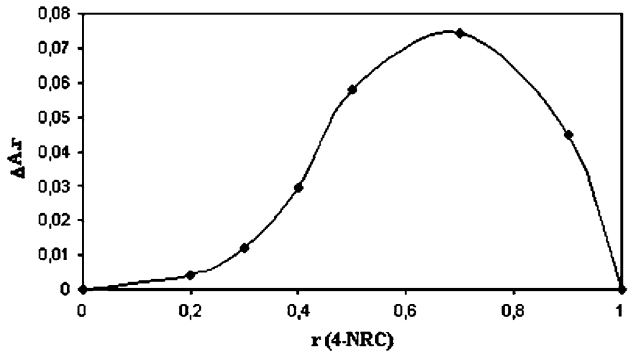

Fig. 3 Job's plot for the complexation of 4-NRC: HP-β-CD system. ΔA = difference of absorbance of 4-NRC at 282 nm with and without HP-β-CD; $r = m/(m + n)$. (m and n are the molar ratios of 4-NRC and HP-β-CD, respectively)

and C=C aromatic stretching bands at 1,635 and 1,522 cm^{-1}, respectively, in addition to an absorption band at 1,283 cm^{-1} related to C–O phenolic strectch.

For the drug–CD physical mixture spectrum (Fig. 4c) the sum of the FTIR spectra of the pure compounds were expected. Although only some 4-NRC aromatic bands were still observed (1,286 cm^{-1} and 1,522 cm^{-1}) while the free ν(OH) and aliphatic bands (2,968 and 1,635 cm^{-1}) were overlapped by ν(–CH/–CH_2) and hydrated bonds of the HP-β-CD bands, all centered at 3,400, 2,930 and 1,654 cm^{-1}, respectively. This could suggest that the phenolic portion of 4-NRC is probably not included (or interacting) in the CD cavity.

Kneading product spectrum (Fig. 4d) showed more intense bands at 3,392, 2,929 and 1,644 cm^{-1} attributed to free –OH, –CH/CH_2 stretching vibration of HP-β-CD. The same correspondent bands were seen in the freeze-dried product (Fig. 4e) at 3,391, 2,930 and 1,654 cm^{-1}, while the ascribed 4-NRC bands at 1,635, 1,522 and 1,245 cm^{-1} have disappeared in both kneading and freeze-dried product. This evidence generally is taken as an indication of the inclusion complex formation [31], although IR spectroscopy is not generally very suitable for unambiguously detecting the inclusion of compounds in CD's, because CD's bands can easily mask the guest's absorptions (*p.e.* different molar ratios between CD/guest compound), especially when there is close related groups, as seen here for both molecules, aside from phenolic group of 4-NRC, which is assigned in a crowded band area of the IR spectra.

Nuclear magnetic resonance characterization

^{1}H-NMR spectrum of cyclodextrin (Fig. 5; Table 1) showed six assignable signals hydrogens H_1, H_2, H_4 being at the outer surface of cyclodextrin, while H_3 and H_5 are facing the interior of CD cavity (the inner surface) and, therefore, they are particularly important for studying host–guest interactions. H_6 is located at the rim of the truncated cone of β-CD with primary alcohols groups, while H_2 and H_4 are at the opposite entrance of the cavity.

Thus, the inclusion of 4-NRC into the HP-β-CD cavity was evaluated by changes in the chemical shifts (δ) of the HP-β-CD hydrogens in the presence and absence of 4-NRC (Fig. 5). Some assignable HP-β-CD and 4-NRC hydrogen atoms, along with the chemical shift deviations due to complexation are presented (Table 1). The H_2 and H_4 hydrogens could not be assigned to HP-β-CD due to signal overlapping in the ^{1}H NMR spectrum. The higher upfield

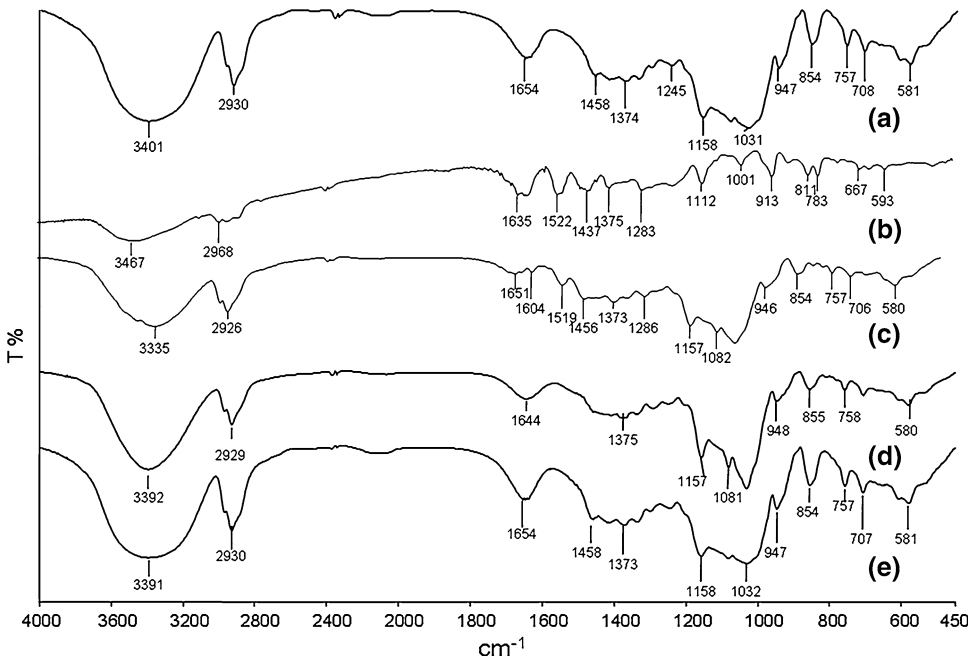

Fig. 4 FT-IR spectra of (**a**) HP-β-CD, (**b**) 4-NRC, (**c**) physical mixture, (**d**) kneaded product, (**e**) inclusion complex

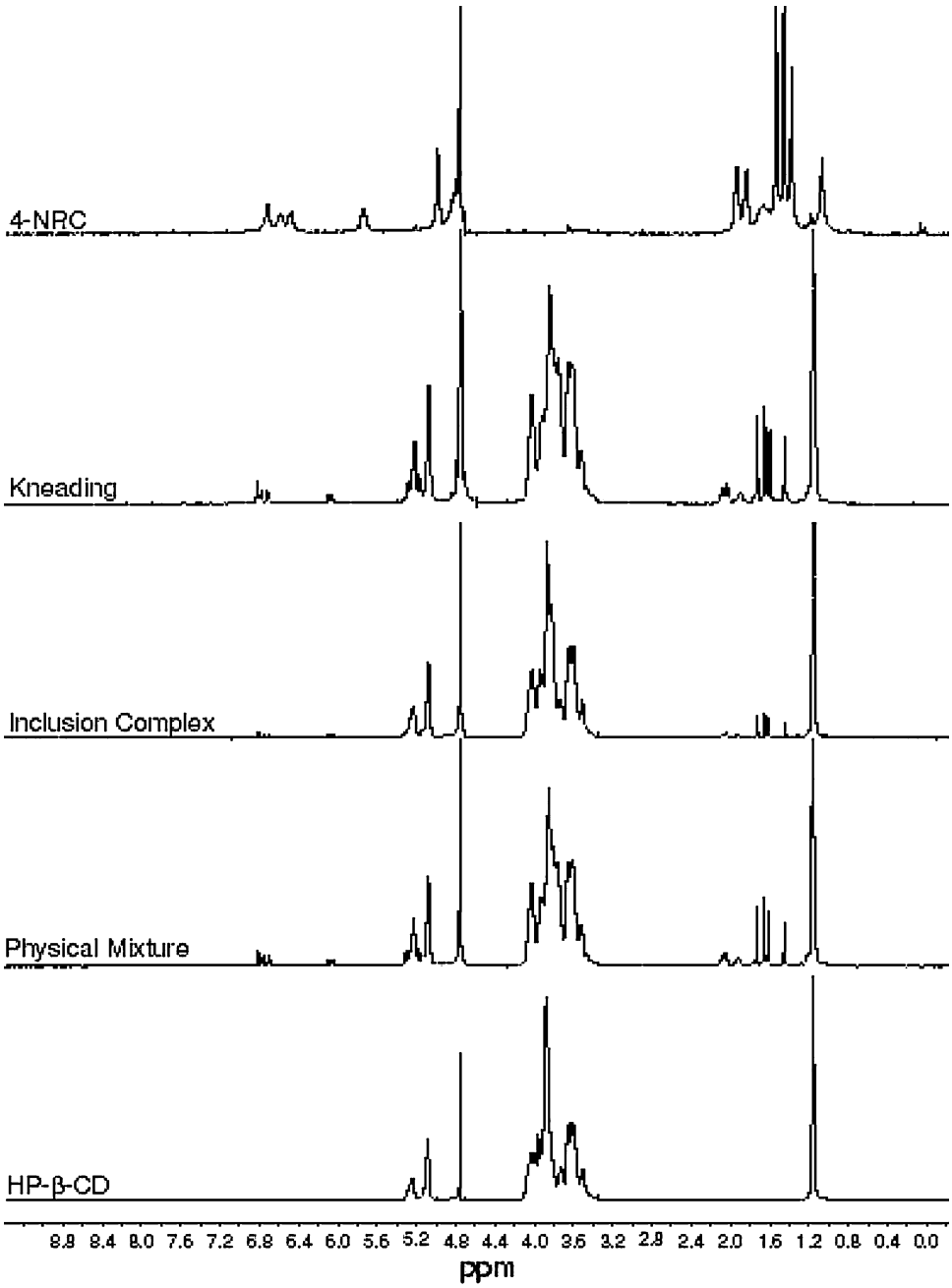

Fig. 5 ^{1}H-RMN spectra of 4-NRC, kneaded product, inclusion complex, physical mixture and HP-β-CD

shifts observed for the internal hydrogens (H_3 and H_5) are indicative that guest molecules (a dimer of 4-NRC) are located close to the hydrogens inside the HP-β-CD cavity for which a shielding is observed [37]. This displacement is due to the anisotropic magnetic effect induced by the presence of the aromatic group of the guest molecule. This strongly shift suggest complexation involving inclusion into the cavity of the host [28], in addition to interactions external to the cavity, as the external hydrogen H_1 was affected, even though to a lesser extent when compared to H_3 and H_5 (Table 1).

The larger shift observed in the presence of 4-NRC for H_5 with respect to H_3, and the significant shift of H_6, indicates that this drug penetrates into the CD cavity from the primary hydroxyl site of the macrocycle. Similar results have been obtained by Ventura et al. [35] and Xinyi and Lindenbaum [38] for chenodeoxycholic acid. The opposite magnitude of H_3 and H_5 shifts in the presence of the guest molecule indicates a probable opposite penetration of the drug. In addition, 4-NRC methylic hydrogens assignable to $C_{12}{}'$, $C_{13}{}'$ and $C_{14}{}'$ and $C_{15}{}'$ were deshielded (Table 1). This can be explained due to hydrogen bonds between HP-β-CD

primary OH groups or glycosidic oxygen atoms and 4-NRC (see discussion item *2:1 Guest: host interactions*).

Molecular modeling studies

Host structures

Primary alcohols of the β-cyclodextrins are involved in hydrogen bonded networks constituted, on average, by the linkages between OH_2 to $OH_{3'}$, OH_3 to $O_{glycosidic}$, OH_2 to $O'_{glycosidic}$, $OH_{3'}$ to $OH_{2'}$, $OH_{2'}$ to $OH_{3''}$, and so successively. The β-CD structure is well described in the literature [39–41], as a truncated cone in which the primary alcohol groups are oriented to the narrower edge, and the secondary hydroxyl groups point toward the wider edge.

Hydroxypropyl chains were added to the secondary alcohol groups of β-CD backbone to form the HP-β-CD guest. Due to their flexibility, a larger movement of those chains would be expected. During dynamic trajectories, one can observe that the tendency of the hydroxyl groups seems to be oriented to the interior of the structure, favouring the hydrogen bond interactions (OH···OH and OH···O_6) and keeping those chains as closed as possible. It can induce a variable effect over the form of the truncated cone. The new defined contour looks like a truncated cylindrical form, measuring around 14.5 Å of width by 11.4 Å of height.

Guest behavior—models for single molecule and for dimer molecules

To cover the molecular movement of 4-NRC, at 298 K, a trajectory of 200 ps was necessary to search the conformational space. A smaller time was not enough to find a folded structure. The six stable conformers chosen to exemplify 4-NRC molecular flexibility are shown in Fig. 6a. Reported energy values correspond to the geometries reoptimized after dynamics. To measure molecular extensions, a pseudo-atom, X_1, was positioned in the center of mass of the aromatic ring. The distances were measured from X_1 to $C_{14'}$ and $C_{15'}$ methyl groups, located in the end of the 4-NRC alkenylated chain. Reported values evaluate the near carbon to the pseudo-atom, and varied from 12.5 Å to 6.9 Å. The most stable geometry, under *vacuum*, got a folded conformation ($E = -31.3$ kcal mol^{-1}) and the energy increment to the longest geometries varies from 1.0 to 2.5 kcal mol^{-1} ($E = -29.4$, -28.4 and -26.9 kcal mol^{-1}).

In order to construct a reasonable approach to model 4-NRC inclusion, a dimer was studied in two different orientations. Two extended conformers, the most stable found from dynamic calculations, were positioned in parallel and in anti-parallel orientations (Fig. 6b).

The starting positions were chosen by visual analysis, optimized and submitted to standard dynamic procedures.

Table 1 ^{1}H-NMR chemical shift displacement ($\Delta\delta$, ppm) of HP-β-CD in freeze-dried product in D_2O

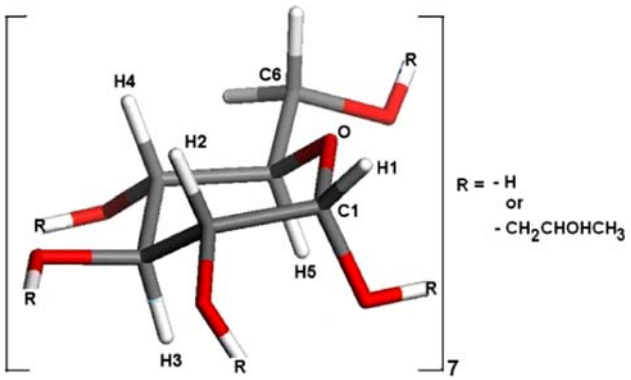

HPβCD	δ free	δ complex	$\Delta\delta$*
H-1	5.08	5.08	0.00
H-2	n.r.	n.r.	n.d.
H-3	3.97	3.94	−0.03
H-4	n.r.	n.r.	n.d.
H-5	3.73	3.72	−0.01
H-6	3.88	3.87	−0.01

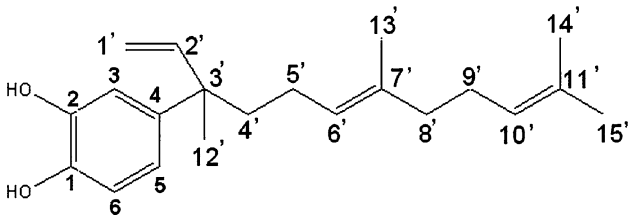

4-NRC	δ free	δ complex	$\Delta\delta$
CH_3 (12′a)	1.07	1,45	+0.38
CH_3 (15′b)	1.38	1,62	+0.24
CH_3 (14′a)	1.46	1,66	+0.20
CH_3 (13′a)	1.54	1,73	+0.19
CH_2 (5; 9′)	1.84; 1.93 (n.r.)	1.95; 2.04 (n.r.)	+0.11; +0.11
CH_2 (4′; 8′)	1.6–1.75 (n.r.)	n.d.	n.d.
CH_2 (1′a; 1′b)	n.d.	n.d.	n.d.
CH_2 (6′; 10′)	4.99 (n.r.)	5.08 (n.r.)	+0.09
CH (2′)	5.73 (n.r.)	6.08 (n.r.)	+0.35
CH (5)	6.48 (n.r.)	n.d.	n.d.
CH (6)	6.59 (n.r.)	6.77 (n.r.)	+0.18
CH (3)	6.72 (n.r.)	6.81 (n.r.)	+0.09

n.r. not resolved; *n.d.* not determined

* $\Delta\delta$ was expressed as $\Delta\delta = \delta_{complex} - \delta_{free}$ CD

In both models the structures stayed together during the trajectory calculations. No important energy variations permit any preference between both models. So, energy values are not valuable criteria in that case. However, the

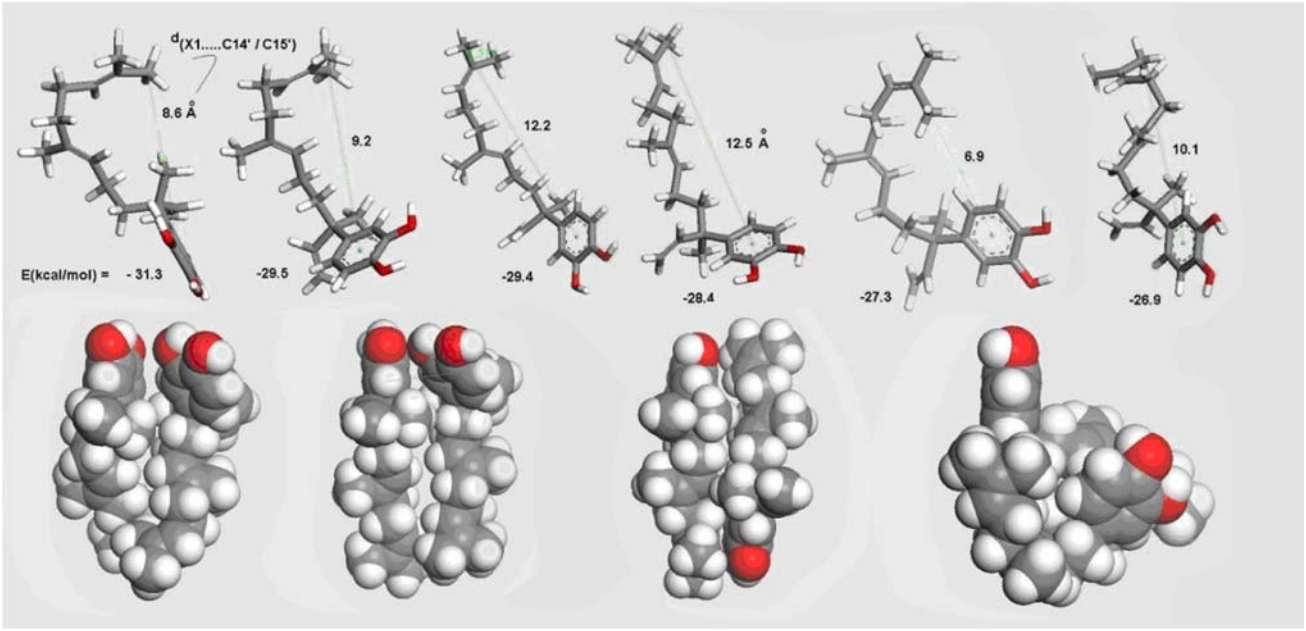

Fig. 6 **a** Six stable conformers representing the 4-NRC conformational space (*up*). **b** Two extended 4-NRC conformers positioned in parallel and in anti-parallel orientations (*down*)

parallel model had a stable dynamic profile, during the observed period of time. The conformations conserved a similar extension ($d_{(X1-C14'/C15')} = 11.1$ Å; 11.7 Å) and the aromatic rings stabilized at a distance of 5.8 Å, measured from their pseudo-atoms.

The second model, in which the 4-NRC molecules were placed in an anti-parallel orientation, seems to be less preferable in those conditions (free molecules and under *vacuum*), because it had taken 140 ps to get a relative stability. It was raised when one molecule had taken a fold conformation, besides the second molecule remained extended ($d_{(X1-C14'/C15')} = 6.7$ Å; 11.1 Å). The collected data are reported in Table 2.

Stoichiometry of the inclusion complex for 4-NRC: cyclodextrin

1:1 Guest: host interactions The complexes were performed following the same strategy. One 4-NRC molecule was included into the cavity, always using the most extended geometry as the initial atomic coordinates set (Fig. 7, models **a**–**d**). Firstly, the pyrocatechol moiety comes into the HP-β-CD cavity by the primary hydroxyl groups side, leaving the isoprenyl chain externally [39, 41]. Then, this aromatic head progressively slides to the HP chains edge. Secondly, the inverse sense of the sliding movement was studied.

We note that calculation procedures are not able to slide ligand in the sense of a translate movement, along the most important HP-β-CD extension (z axis). This movement was reproduced by many models, and we are discussing only the most significant among them. The guest is extremely stable in all situations. As the cavity is large, it comes easily in and is stabilized mainly by electrostatic interactions. The two OH (phenolic) groups of 4-NRC may form an intramolecular hydrogen bond and another one with HP-β-CD external OH groups. They are good models to verify the short distance interactions among OH groups of aromatic ring and H_3 and/or H_5 of HP-β-CD, as well as the C_1' and C_{12}', C_{13}' and C_{14}'/C_{15}' methyl groups of 4-NRC molecule (Fig. 1a). The most difficult interactions to be verified are the ones involving $C_{14'}/C_{15'}$ methyl groups, because they are dependent of the 4-NRC chains movement. To do that, the chain needs to be folded, as a "u" form, to turn those methyl groups toward the HP chains. Those movements take at least 145 ps to be reached and stabilized.

There is no energetic difference when 4-NRC enter from the one or another side of the host, and stay in an almost extended conformation (Fig. 7, models **a** and **c**). Those orientations do not favour the interactions among $C_{14'}/C_{15'}$ methyl groups of 4-NRC and the host. Due to the multiple HP-β-CD intramolecular hydrogen bonds formed during movement in those guest conformations, the complexes keep their truncated cylinder shape.

Nevertheless, when the guest (phenolic side) is stabilized almost in the middle of the host, the alkenyl chain is particularly lengthy and stays outside enough to be folded and the extreme methyl groups might interact with HP-β-CD (Fig. 7, models **b** and **d**). The minimum energy was

Table 2 Structural data, Connolly occupied volume and surface area calculated for all discussed models

Models	E_{tot} (kcal mol^{-1})	Connolly surface		$d_{(X1-C14'/C15')}$ (Å)*
		Occupied volume (Å^3)	Surface area (Å^2)	
Initial and host structures				
β-CD	−177.0	1020.29	865.73	–
HP-β-CD	−431.9	1514.14	1220.52	–
Study for flexibility and shape complementarities for a single 4-NRC molecule and for a dimer				
4-NRC (folded conformation)	−31.3	359.49	362.03	8.6
4-NRC (extended conformation)	−29.4	354.80	371.41	12.2
4-NRC—dimer in parallel orientation	−94.1	749.17	684.45	11.1/11.7
4-NRC—dimer in anti-parallel orientation	−94.7	751.62	655.28	6.7/11.1
Inclusion—single 4-NRC				
C*atechol-in* by 1^{ary} OH side—model **a**	−547.4	1510.22 (HpβCD)	1250.77	11.5
		356.66 (4-NRC)	359.77	
		1978.27 (both)	1292.96	
Catechol-in by 1^{ary} OH side—model **b**	−584.0	1514.58 (HpβCD)	1251.73	10.0
		361.81 (4-NRC)	354.81	
		1970.91 (both)	1350.38	
Catechol-in by HP side—model **c**	−547.8	1523.02 (HpβCD)	1206.40	11.8
		357.20 (4-NRC)	359.40	
		1909.38 (both)	1274.89	
Catechol-in by HP side—model **d**	−570.1	1510.83 (HpβCD)	1241.49	8.0
		358.86 (4-NRC)	376.75	
		1967.91 (both)	1429.0	
Inclusion—4-NRC dimmer				
Catechol moieties turned to host centre—model **e**, conformation **a**	−641.2	1519.57 (HpβCD)	1289.73	8.3/9.7
		727.72 (4-NRC's)	694.51	
		2365.25 (all)	1604.52	
Catechol moieties turned to host centre—model **e**, conformation **b**	−693.0	1523.67 (HpβCD)	1303.54	8.5/9.6
		732.82 (4-NRC's)	690.58	
		2368.89 (all)	1576.84	
Parallel orientation—model **f**	−541.2	1504.39 (HpβCD)	1302.53	12.1/8.5
		722.87 (4-NRC's)	611.32	
		2322.28 (all)	1418.05	
Anti-parallel orientation—model **g**	−617.2	1509.55 (HpβCD)	1275.69	8.4/13.1
		730.23 (4-NRC's)	634.93	
		2365.10 (all)	1459.58	
Parallel orientation, catechol moieties out of HP side—model **h**	−621.7	1510.93 (HpβCD)	1331.76	12.5/12.9
		746.27 (4-NRC's)	620.82	
		2391.23 (all)	1406.04	
Parallel orientation, catechol moieties out of 1^{ary} OH side—model **i**	−625.3	1515.14 (HpβCD)	1356.05	10.8/12.7
		741.60 (4-NRC's)	649.91	
		2376.83 (all)	1523.29	
Anti-parallel orientation, catechol moieties are out of HP-β-CD, aliphatic chains are fully inside—model **j**	−631.9	1512.33 (HpβCD)	1331.66	12.6/12.9
		729.31 (4-NRC's)	647.39	
		2371.56 (all)	1443.73	

* The distances were measured from the pseudo-atom of the catechol moiety to the nearest C14′ or C15′ methyl group located in the end of 4-NRC chain

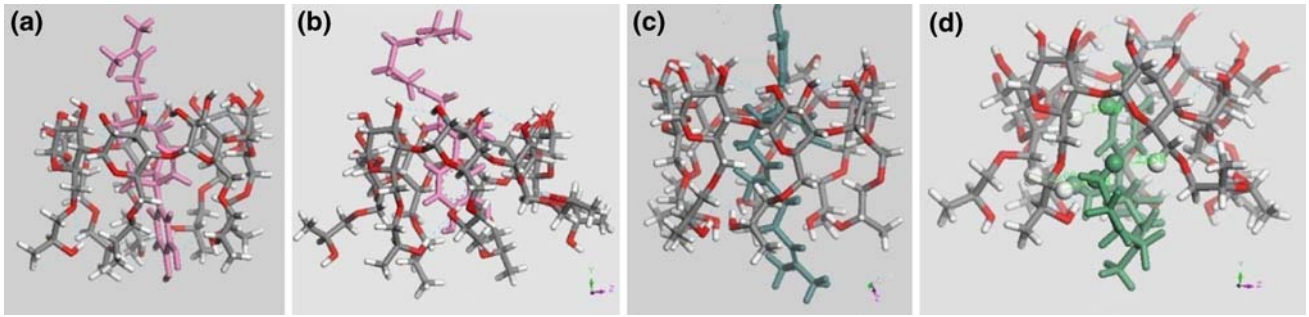

Fig. 7 Inclusion of a single 4-NRC molecule in two directions. Pyrocatechol comes into the cavity from primary hydroxyl groups (models **a**, **b**) or from hydroxypropyl side chains (models **c**, **d**). The most stable orientation was reached when the 2-hydroxylphenol ring stabilizes in a medium position of HP-β-CD cavity (model **b**)

obtained for that middle position of catechol ring, when the 4-NRC isoprenyl side chain is folded over the primary hydroxyl groups. In model **b**, 15 hydrogen bonds stabilize the inclusion complex. Also, four short distance interactions were measured between the phenolic groups OH_1 and OH_2, $H_{1'}$ and $H_{12'}$, whose interactions are with a OH and a hydrogen atom from two HP chains, and with H_3 atoms from two different glucose monomers of the β-CD moiety. The overall form of the host changes once again, to become a truncated cone. The narrow edge is formed by the OH groups of β-CD side and the wider edge formed by the HP chain side. That was clearly the most stable complex for a single 4-NRC inclusion and the energy value was largely lower than the other ones ($E_{(\text{model } \mathbf{b})} = -584.0$ kcal $\cdot$ mol^{-1}) (Table 2).

2:1 Guest: host interactions Experimental results gave a stoichiometric relationship of two 4-NRC molecules to one HP-β-CD molecule [42]. Carefully our study was driven to this direction. The next computational steps were carried out to verify the adaptation, best orientation, stability, electrostatic and hydrogen bond interactions among two guests—a dimer and one host molecules.

Two 4-NRC molecules were inserted into the cavity following the knowledge about molecular behavior raised previously. In the first dimer model for inclusion (Fig. 8, model **e**), the ligand molecules were introduced in their extended form, the two catechol moieties turned to the center of the host, taking the best orientation reached through the model **b**, explained on previous section.

Two system conformations (Fig. 8, cf. **a** and cf. **b**) were found during dynamic trajectory, with a significant energy variation of 52 kcal mol^{-1}. The most stable system was reached when both 4-NRC alkenyl chains were folded enough to interact with the extremities of the host, at around 2.5 Å. The centre of mass of the catechol aromatic rings stabilizes at a distance of 4.1 Å (Fig. 8, cf. **b**) and with the lower energy value found in this study. Further dynamic simulations confirm the high molecular system stability, with no significant changes in the reported complex conformation.

Due to their relative positions and electrostatic interactions, the phenolic groups of 4-NRC remain close, inducing a slight ring distortion to their planarity. Those distortions were not corrected by calculations in spite of the energetic gradient convergence until 1.0×10^{-5} kcal mol^{-1} Å^{-1}. The short distance interactions among phenolic OH_1 and OH_2 and hydrogen atoms H_2, H_3 and/or H_5 of HP-β-CD, as well as the $C_{1'}$ hydrogen atoms, and the methyl groups $C_{12'}$, $C_{13'}$ and $C_{14'}/C_{15'}$ of 4-NRC molecule were also verified and measured. A first series of measurements made from

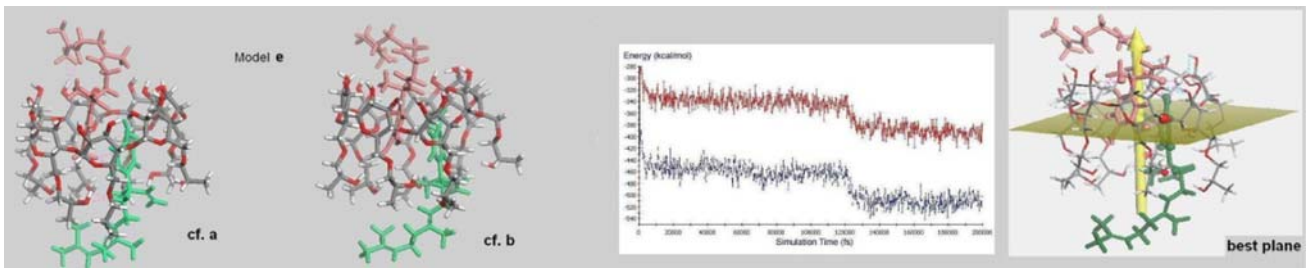

Fig. 8 Inclusion of a 4-NRC dimer in two opposite directions, the pyrocatechol rings stabilized almost in the middle of the cavity. Two stable conformations of the complex were clearly formed—(model **e**, cf. **a**) $E = -641.2$ kcal mol^{-1}; (model **e**, cf. **b**) $E = -693.0$ kcal mol^{-1})—as it is shown during dynamic trajectory at 298 K, for 200 ps. The best plane shows that relative position of the two pyrocatechol moieties, in the centre of HP-β-CD cavity

one of the 4-NRC molecules (magenta colour in Fig. 8) show eight important steric proximities between 4-NRC and six different glucose monomers: phenolic $OH_1\cdots H_5$ (2.37 Å) and phenyl $H_6\cdots O_{intracyclic}$ (2.38 Å) (with the same glucose monomer); phenolic $OH_2\cdots O_{glycosidic}$ (2.24 Å); $H_{2'}\cdots OH_2$ (1.92 Å); one hydrogen atom of methyl $C_{12'}\cdots H_3$ (1.89 Å), and, finally, $C_{13'}$, $C_{14'}/C_{15'}$ interact with OH_3 coming from three different glucose rings (2.35 Å, 2.43 and 3.24 Å). The second series of measurements made from the second 4-NRC molecule (green colour in Fig. 8) and HP-β-CD show seven important steric proximities, involving five glucose monomers: phenolic $OH_1\cdots H_3$ (1.74 Å) and $OH_1\cdots H_2$ (2.42 Å); $H_{5(phenyl)}\cdots H_{5(glucose)}$ and $H_{6(phenyl)}\cdots H_{5(same\ monomer)}$ (2.13 and 2.36 Å); $H_{1'}\cdots OH_5$ (1.91 Å); $H_{3(phenyl)}\cdots OH_{5(glucose)}$ (2.22 Å) and one H atom of $C_{12'}\cdots H_3$ (1.89 Å). Six hydrogen bonds formed between primary hydroxyl groups or glycosidic oxygen atoms and two others formed between HP hydroxyl groups contribute to the system stability. As a reference frame for the relative molecular orientation of that model, the best plane and its central axe were calculated and represented in Fig. 8.

Two 4-NRC molecules were then inserted together into the cavity, firstly in a parallel orientation (Fig. 9, models **f**, **h** and **i**), than in an anti-parallel orientation (Fig. 9, models **g** and **j**). Their adaptation in the cavity is quite unbelievable, and they seem to have naturally the necessary movements to fit the cavity without significant distortion over the full HP-β-CD structure. As unreal as it looks like, both guest molecules seem to fit very comfortably, and to be absorbed by this strongly lipophilic and cylindrical tunnel.

For model **f** (Fig. 9), in which guests are in parallel orientation, the aromatic centres of catechol slide one from another, stabilizing at 3.7 Å. Isoprenyl chains found an extended and a folding conformation and turns toward the HP host chains. The dynamic trajectory had shown a very stable system. A few picoseconds were necessary to the complex to find a good complementarity among them, and the three molecules composing the complex remain extended, one throughout the others. Nevertheless, in spite of the good molecular complementarity and very strong stability during dynamics, this complex presented the most important energetic value among the dimer models ($E = -541.2$ kcal mol^{-1}).

In spite of still describing a parallel orientation for the guests, the models **h** and **i** are slightly different because the 4-NRC isoprenyl chains where fully inserted into the cylinder, instead of the catechol moieties, which were located almost outside of the HP-β-CD molecular core. When insertion kept the head of catechol moieties near the HP side chains, the aromatic rings stabilize in a distance of 4.2 Å, considering their centre of mass (Fig. 9, model **h**). Fifteen picoseconds had been necessary to stabilize the system and further fluctuations did not introduce significant system changes.

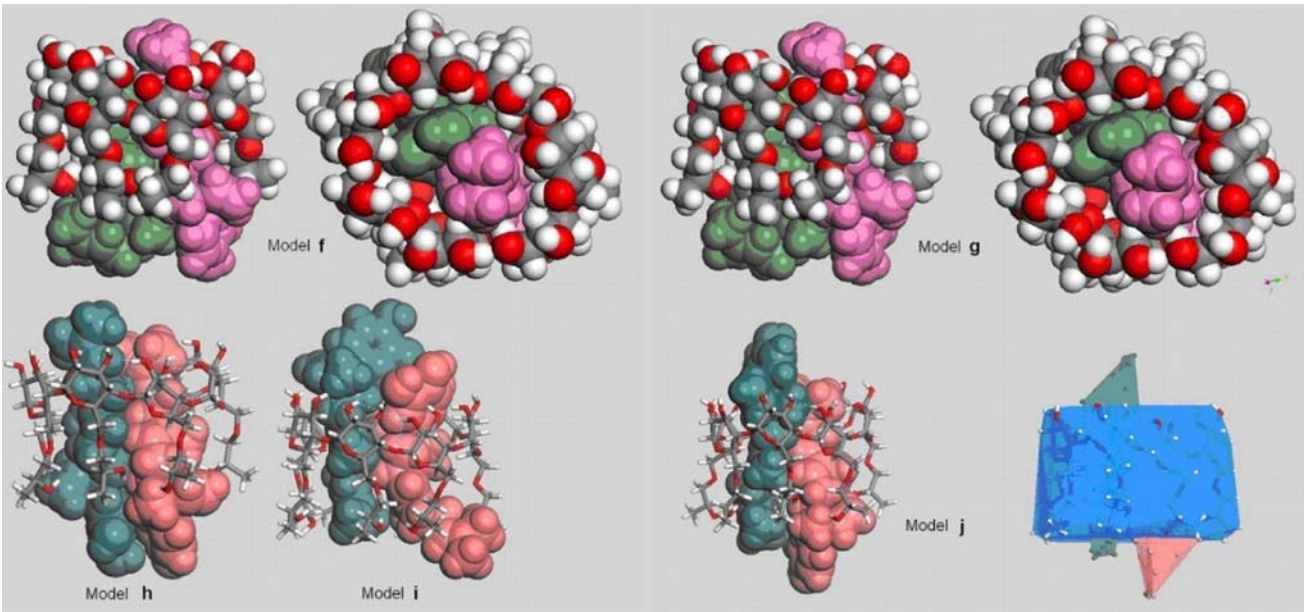

Fig. 9 (*Left*) 4-NRC dimer inclusion in parallel orientations (*up row*: model **f**; *down*: models **h** and **i**). The snapshots show the guests adaptation into the host cavity. (*Right*) 4-NRC dimer inclusions in anti-parallel orientation. The snapshots show the guests adaptation into the host cavity (*up row*: model **g**; *down*: model **j**). The *polyhedrons* show that the truncated cone representing the HP-β-CD structure is appropriate for model **i**

When guests were inserted from the primary OH side of the host, the aromatic rings stabilize in a distance of 5.6 Å (Fig. 9, model **i**). Thirty picoseconds (30 ps) had been necessary to slide these aromatic catechol rings, to fold one of the guest alkenyl chain and to stabilize the system ($E = -621.7$ and -625.3 kcal mol^{-1}, respectively).

Once again, the results based on the energy variation show that it has no significant difference for guest insertions, when the aromatic rings stay near the primary OH host side, or near the HP side chains. Nevertheless, the 4-NRC dimer seems to be able to stay in an extended conformation and very close one to other when the catechol aromatic rings are located near the primary OH groups.

For the anti-parallel model **g** (Fig. 9), the molecules found their complementarities after almost 20 ps and the later fluctuations represented just minor adjustments. The aromatic centres of catechol are displaced by 10.2 Å. One 4-NRC molecule conformation is folded; its aromatic ring stabilizes into the cavity. Another is extended, the HP chains had been opened allowing this guest aromatic ring to be exposed to the outside, decreasing probably steric hindrance.

Model **g** volume is somewhat bigger than model **f**, its homologue in the parallel orientation (Fig. 8; Table 2) and presents a lower energy value than model **f** ($E = -617.2$ and -541.2 kcal mol^{-1}, respectively). Their energy variation amount ($\Delta E = 76.0$ kcal mol^{-1}) is almost the same as that found between model **g** and model **e**, cf. **b**, which has the two catechol moieties positioned in the middle of the host cavity ($E = -617.2$ and -693.0 kcal mol^{-1}, respectively).

Our last model, **j,** in which catechol moieties remain both in opposite direction, showed a very stable dynamic profile. Guest molecules stayed in an extended form, the alkenyl chains are perfectly adapted one to another and they are also well adapted, stabilized and fully inserted into the core of host molecule. Catechol rings are mainly exposed to the outside of host molecule. This system **j** is more stable ($E = -631.9$ kcal mol^{-1}) than all other inclusion complexes of two 4-NRC molecules, excepting model **e**.

Finally, comparison of all models confirms that the guest dimer, in an antiparallel orientation is preferred, independent of the catechol moieties position, which could be located fully into the host cavity or outside, without significant increase in energy for the molecular system. Besides, the hydrogen bond network, the low molecular system energy, the steric interactions and the good agreement with the upfield and downfield chemical shift displacements observed in ^{1}H NMR spectra gave us precise data to confirm model **e**, conformation **b**, as the best model for the dimer guest:HP-β-CD host complexation.

Conclusions

This study presented the preparation and physicochemical characterization for the 4-NRC: HP-β-CD inclusion complex. The results indicated a stable 4-NRC: HP-β-CD complex ($K_a = 6494 \pm 837$ M^{-1}) and a stoichiometry of complexation of 2:1 (4-NRC: HP-β-CD). All data obtained from UV–Vis, FT-IR, ^{1}H NMR techniques support the formation of the inclusion complex. Molecular modeling studies confirm the stoichiometry of the complex and showed that two guests molecules are in an anti-parallel orientation and their pyrocatechol groups are positioned in the middle of the host cavity. 4-NRC complexation indeed led to higher drug stability and could probably be useful to improve its biological properties (antioxidant, analgesic, anti-inflammatory and others) and make it available for oral administration and topical formulations. In vivo studies of the complexes are in progress to evaluate the effect of CDs on bioavailability and pharmacological activity of the drug.

Acknowledgments This work was partly supported by a grant from CNPq and SECTEC-GO. The authors acknowledge Dr. Massayoshi Yoshida and Dr. Luiz Carlos Roque for the NMR 500 MHz data acquisition. We are especially grateful to Prof. Harry Pearson for English corrections on the manuscript.

References

1. Ropke, C.D., da Silva, V.V., Kera, C.Z., Miranda, D.V., de Almeida, R.L., Sawada, T.C., Barros, S.B.M.: In vitro and in vivo inhibition of skin matrix metalloproteinases by *pothomorphe umbellata* root extract. Photochem. Photobiol. **82**(2), 439–442 (2006)
2. Ropke, C.D., Kaneko, T.M., Rodrigues, R.M., Silva, V.V., Barros, S., Sawada, T.C.H., Kato, M.J., Barros, S.B.M.: Evaluation of percutaneous absorption of 4-nerolidylcathecol from four topical formulations. Int. J. Pharm. **249**(1–2), 109–116 (2002)
3. Ropke, C.D., Meirelles, R.R., Silva, V.V., Sawada, T.C.H., Barros, S.B.M.: *Pothomorphe umbellata* extract prevents α-tocopherol depletion after UV-irradiation. Photochem. Photobiol. **78**(5), 436–439 (2003)
4. Ropke, C.D., Sawada, T.C.H., da Silva, V.V., Michalany, N.S., Barros, S.B.M.: Photoprotective effect of *Pothomorphe umbellata* root extract against ultraviolet radiation induced chronic skin damage in the hairless mouse. Clin. Exp. Dermatol. **30**(3), 272–276 (2005)
5. Barros, S.B.M., Ropke, C.D.: Use of *Pothomorphe umbellata* extract, composition on basis of *Pothomorphe umbellata* extract and method of application on the *Pothomorphe umbellata* extract. (Fundação de Amparo a Pesquisa do Estado de São Paulo—FAPESP, Brazil; Universidade de São Paulo—USP). PCT Int. Appl. (2004), CODEN: PIXXD2 WO 2004026323 A1
6. Perazzo, F.F., Souza, G.H.B., Lopes, W., Cardoso, L.G.V., Carvalho, J.C.T., Nanayakkara, N.P.D., Bastos, J.K.: Anti-inflammatory and analgesic properties of water–ethanolic extract from *Pothomorphe umbellata* (Piperaceae) aerial parts. J. Ethnopharmacol. **99**(2), 215–220 (2005)

7. Mongelli, E., Desmarchelier, F., Coussio, J., Ciccia, G.: Antimicrobial activity and interaction with DNA of medicinal plants from the Peruvian Amazon region. Rev. Argent. Microbiol. **27**(4), 199–203 (1995)
8. Mongelli, E., Romano, A., Desmarchelier, C., Coussio, J., Ciccia, G.: A cytotoxic catechol derivative from *Pothomorphe peltata* inhibits topoisomerase I activity. Planta Med. **65**(4), 376–378 (1999)
9. Valadares, M.C., Rezende, K.R., Pereira, E.R., Sousa, M.C., Gonçalves, B., de Assis, J.C., Kato, M.J.: Protective effects of 4-nerolidylcatechol against genotoxicity induced by cyclophosphamide. Food Chem. Toxicol. **45**(10), 1975–1978 (2007)
10. Vandelli, M.A., Salvioli, G., Mucci, A., Panini, R., Malmusi, L.: 2-Hydroxypropyl-β-cyclodextrin complexation with ursodeoxycholic acid. Int. J. Pharm. **118**(1), 77–83 (1995)
11. Fernandes, C.M., Vieira, M.T., Veiga, F.J.B.: Physicochemical characterization and in vitro dissolution behavior of nicardipine–cyclodextrins inclusion compounds. Eur. J. Pharm. Sci. **15**(1), 79–88 (2002)
12. Archontaki, H.A., Vertzoni, M.V., Athanassiou-Malaki, M.H.: Study on the inclusion complexes of bromazepam with β- and β-hydroxypropyl-cyclodextrins. J. Pharm. Biomed. Anal. **28**(3–4), 761–769 (2002)
13. Duchêne, D., Wouessidjewe, D.: Pharmaceutical uses of cyclodextrins and derivatives. Drug Dev. Ind. Pharm. **16**(17), 2487–2499 (1990)
14. Leroy-Lechat, F., Wouessidjewe, D., Andreux, J.P., Puisieux, F., Duchêne, D.: Evaluation of the cytotoxicity of cyclodextrins and hydroxypropylated derivatives. Int. J. Pharm. **101**(1–2), 97–103 (1994)
15. Davis, M.E., Brewster, M.E.: Cyclodextrin-based pharmaceutics: past, present and future. Nat. Rev. Drug Discov. **3**(12), 1023–1035 (2004)
16. Hirsch, W., Fried, V., Altman, L.: Effect of cyclodextrins on sparingly soluble salts. J. Pharm. Sci. **74**(10), 1123–1125 (1985)
17. Rezende, K.R., Barros, S.B.M.: Quantification of 4-nerolidylchatecol of *Pothomorphe umbellata* (Piperaceae) in rat plasma samples by HPLC UV. Braz. J. Pharm. Sci. **40**(3), 373–380 (2004)
18. Gustafson, K.R., Cardellina, J.H., McMahon, J.B., Pannell, L.K., Cragg, G.M., Boyd, M.R.: The peltatolls, nove HIV-inhibitory catechol derivates from *P. peltata*. J. Org. Chem. **57**(10), 2809–2811 (1992)
19. Higuchi, T., Connors, K.A.: Phase solubility techniques. Adv. Anal. Chem. Instrum. **4**, 117–212 (1965)
20. Job, P.: Formation and stability of inorganic complexes in solution. Ann. Chim. **9**, 113–203 (1928)
21. Calabro, M.L., Tommasini, S., Donato, P., Ranieri, D., Stancanelli, R., Ficarra, P., Ficarra, R., Costa, C., Catania, S., Rustichelli, C., Gamberini, G.: Effects of α- and β-cyclodextrin complexation on the physico-chemical properties and antioxidant activity of some 3-hydroxyflavones. J. Pharm. Biomed. Anal. **35**(2), 364–367 (2004)
22. Materials Studio Software and Insight II Software, Accelrys, 9685 Scranton Road, San Diego, CA 92121-3752, USA
23. Hwang, M.J., Stockfisch, T.P., Hagler, A.T.: Derivation of Class II force fields. 2. Derivation and characterization of a Class II force field, CFF93, for the alkyl functional group and alkane molecules. J. Am. Chem. Soc. **116**(6), 2515–2525 (1994)
24. Sun, H., Mumby, S.J., Maple, J.R., Hagler, A.T.: An ab initio CFF93 all-atom force field for polycarbonates. J. Am. Chem. Soc. **116**(7), 2978–2987 (1994)
25. Abola, E.E., Bernstein, F.C., Bryant, S.H., Koetzle, T.F., Weng, J., Allen, F.H., Bergerhoff, G., Sievers, R.: Protein Data Bank. In Allen, F.H., Bergerhoff, G., Sievers, R. (eds.) Crystallographic Databases—Information Content, Software Systems, Scientific Applications. Data Commission of International Union of Crystallography, Cambridge (1987)
26. Berman, H.M., Westbrook, J., Feng, Z., Gilliland, G., Bhat, T.N., Weissig, H., Shindyalov, I.N., Bourne, P.E.: The protein Data Bank. Nucleic Acids Res. **28**, 235–242 (2000) http://www.rcsb.org/PDB. Accessed 12 June 2008
27. Sharff, A.J., Rodseth, L.E., Quiocho, F.A.: Refined 1.8-.ANG. structure reveals the mode of binding of beta-cyclodextrin to the maltodextrin binding protein. Biochemistry **32**(40), 10553–10559 (1993)
28. Connolly, M.L.: Solvent-accessible surfaces of proteins and nucleic acids. Science **221**(4612), 709–713 (1983)
29. Connolly, M.L.: Shape distributions of protein topography. Biopolymers **32**(9), 1215–1236 (1992)
30. Loftsson, T., Brewster, E.M.: Pharmaceutical applications of cyclodextrins. 1. Drug solubilization and stabilization. Int. J. Pharm. Sci. **85**(10), 1017–1025 (1996)
31. Imonigie, J.A., Macartney, D.H.: Effects of cyclodextrin inclusion on the kinetics on the outer-sphere oxidation of 4-tert-butylcatechol by transition metal complexes in acidic aqueous media. Inorg. Chem. **32**(6), 1007–1012 (1993)
32. Tønnesen, H.H., Másson, M., Loftsson, T.: Studies of curcumin and curcuminoids. XXVII. Cyclodextrin complexation: solubility, chemical and photochemical stability. Int. J. Pharm. **244**(1–2), 127–135 (2002)
33. Blanco, J., Vila-Jato, J.L., Otero, F., Anguiano, S.: Influence of method of preparation on inclusion complexes of naproxen with different cyclodextrins. Drug. Dev. Ind. Pharm. **17**(7), 943–945 (1991)
34. Pitha, J., Milecki, J., Fales, H., Pannell, L., Uekama, K.: Hydroxypropyl-β-cyclodextrin: preparation and characterization; effects on solubility of drugs. Int. J. Pharm. **29**(1), 73–82 (1986)
35. Ventura, C.A., Tirendi, S., Puglisi, G., Bousquet, E., Panza, L.: Solid-state properties of powders in the formulation and processing of solid dosage forms. Int. J. Pharm. **14**(1), 1–13 (1997)
36. Sacoman, J.L., Monteiro, K.M., Possenti, A., Figueira, G.M., Foglio, M.A., Carvalho, J.E.: Cytotoxicity and antitumoral activity of dichloromethane extract and its fractions from *Pothomorphe umbellata*. Braz. J. Med. Biol. Res. **41**(5), 411–415 (2008)
37. Gibaud, S., Zirar, S.B., Mutzenhardt, P., Fries, I., Astier, A.: Melarsoprol–cyclodextrins inclusion complexes. Int. J. Pharm. **306**(1–2), 107–121 (2005)
38. Xinyi, T., Lindenbaum, S.: Studies on complexation between β-cyclodextrin and bile salts. Int. J. Pharm. **74**(1–2), 127–135 (1991)
39. Veiga, F.J.B., Fernandes, C.M., Carvalho, R.A., Geraldes, C.F.G.C.: Molecular modeling and 1H-NMR: ultimate tools for the investigation of tolbutamide: β-cyclodextrin and tolbutamide: hydropropyl-β-cyclodextrin complexes. Chem. Pharm. Bull. **49**(10), 1251–1256 (2001)
40. Martin Del Valle, E.M.: Cyclodextrins and their uses: a review. Process Biochem. **39**(9), 1033–1046 (2004)
41. Araujo, M.V.G., Vieira, E.K.B., Lázaro, G.S., Conegero, L.S., Ferreira, O.P., Almeida, L.E., Barreto, L.S., Costa Junior, N.B.C., Gimenez, I.F.: Inclusion complexes of pyrimethamine in 2-hydroxypropyl-β-cyclodextrin: characterization, phase solubility and molecular modelling. Bioorg. Med. Chem. **15**(17), 5752–5759 (2007)
42. Soares, L.A.: Preparação e caracterização do complexo de inclusão do 4-nerolidilcatecol em hidroxipropil-β-ciclodextrina. M.Sc. Thesis, Universidade Federal de Goiás, Goiânia, GO (2007)